Chapter 2

A conserved parasite-specific insert is a key regulator of the activities and interdomain interactions of *Plasmodium falciparum* AdoMetDC/ODC

2.1. Introduction

ODC and AdoMetDC are rate-limiting enzymes in the polyamine biosynthetic pathway and in *P. falciparum* are uniquely located on one polypeptide encoded by a single open reading frame to form a ~330 kDa heterotetrameric, bifunctional *Pf*AdoMetDC/ODC complex [70]. The heterotetrameric nature is due to an autocatalytic processing event within the *Pf*AdoMetDC domain of one *Pf*AdoMetDC/ODC polypeptide, resulting in the formation of two non-identical α- and β-subunits with the essential pyruvoyl moiety covalently bound to the N-terminus of the α-subunit for catalysis [70]. Although the two decarboxylase activities of the bifunctional complex can function independently [71], inter- and intradomain interactions have been shown to stabilise the active bifunctional *Pf*AdoMetDC/ODC complex while unique parasite-specific inserts within the two domains mediate these physical interactions and thereby regulate the activities of both domains [69]. The interdomain interactions therefore support a proposed regulatory mechanism of both decarboxylase activities within the bifunctional complex, which has not been experimentally investigated. Recently, it was shown that an N-terminal non-homologous insert of *P. falciparum* hydroxymethylpterin pyrophosphokinase/dihydropteroate synthase, which is not located within the active site, affects the activities of both enzymes and it was suggested that this insert could be involved in the interaction of the two catalytic domains of the bifunctional complex [133].

The *Pf*ODC domain occurs at the C-terminus of the bifunctional protein and includes residues 805-1419. The protein contains regions of homology to mammalian ODC, especially concerning the residues involved with co-factor binding and catalytic activity as well as several quaternary structural features. These regions of homology are interspersed with parasite-specific inserts [69,70]. Similar to other eukaryotes, the activity of *Pf*ODC is dependent on the formation of a homodimer, where the two active sites are formed by residues contributed from both monomers at the dimer interface. The aromatic Phe1392, Tyr1305 and Phe1319 residues form hydrophobic contacts across the dimer interface, which result in an antiparallel-stacked interaction. A number of studies have investigated features of ODC such as the contribution of long-range interactions

mediated by residues distant from the active site in the promotion of catalytic efficiency (Lys294 of *T. brucei*) [134] and the rapid exchange of mammalian ODC subunits [23]. In the latter study it was shown the active sites consisted of Lys69, Lys169 and His197 (from one subunit) and Cys360 (from the second subunit). Subsequent mutagenesis of these residues and mixing of the mutated monomer with a wild-type one resulted in a rapid exchange of subunits between the enzyme dimers at physiological conditions. The authors suggested that the rapid association and dissociation of ODC facilitates antizyme binding and thus the short half-life of ODC *in vivo* [23].

Comparison of the residues involved in PLP binding of *Pf*ODC to those of *T. brucei* and human ODC (Cys1355, Asp887, Arg955, His998, Ser1001, Gly1037, Gly1114, Gly1116, and Tyr1384, numbered according to the bifunctional protein) showed only three unique residues for *Pf*ODC PLP binding, while two residues were also specific in *Pf*ODC substrate binding (Tyr966 and Arg1117) [127]. Subsequent mutagenesis studies of these residues confirmed their importance in both PLP and substrate binding. These unique properties provide important starting points for the identification of compounds that could be used to selectively target the plasmodial enzyme in an otherwise highly conserved protein.

2.1.1. Parasite-specific inserts within the polyamine biosynthetic enzymes of *P. falciparum*

Compared to the size of the independent monofunctional AdoMetDC and ODC orthologues in humans, the size of the *Pf*AdoMetDC/ODC bifunctional protein is much larger than just the combination of these proteins. This is due to the presence of several parasite-specific inserts within both of the domains that interrupt sequence homology [69,120,127] and, excluding the contribution of the hinge region, increases the size of *Pf*AdoMetDC/ODC by 366 residues (~40 kDa).

Parasite-specific inserts are an interesting feature of plasmodial proteins that form long insertions separating well-conserved blocks that are adjacent in the homologous proteins [135]. These inserts can be present as tandem repeats or sparsely distributed insertions between globular domains and show species-specific characteristics such as rapid divergence, non-globularity and low-complexity. The inserts are mostly flexible and hydrophilic due to the high abundance of Asn and Lys residues, which form loops on the surface of the protein. The frequency of low-complexity regions (subsequences of biased composition) in parasite-specific inserts in *P. falciparum* proteins is particularly high and can be found in enzymes such as RNA polymerases [136], glutamylcysteine synthetase [137], DHFR/TS [138] and DNA topoisomerase [139]. It has

been hypothesised that these low-complexity regions in proteins may promote protein-protein interactions [140] and their high prevalence within *P. falciparum* proteins raises questions about their origin and maintenance within the parasite genome as well as influence on the evolution of the parasite's unusual genome [135,141,142]. Furthermore, these inherently flexible protein elements that do not spontaneously fold into stable globular structures and are often characterised as intrinsically unstructured [143,144], may allow the proteins to recognise several biological targets by becoming structured upon interaction with specific targets [145]. A recent study to identify intrinsically unstructured proteins in the *P. falciparum* proteome showed a high correlation between the presence of these large segments of disordered structures in proteins that play a role in host-parasite interactions (specifically in the sporozoite life cycle stage) [143] as well as in proteins that self-assemble into large multiprotein complexes [140].

Both the *Pf*AdoMetDC and *Pf*ODC domains contain parasite-specific inserts that disrupt regions of homology and range in size from 6 to 180 residues [120,127]. The *Pf*AdoMetDC domain contains three inserts (A1: residues 57-63; A2: residues 110-137; and A3: residues 259-408) [120]. The hinge occupies residues 530-804 and is for all purposes also considered as an insert, while two inserts are present in the *Pf*ODC domain (O1: residues 1047-1085 and O2: residues 1156-1302) [127]. Although the roles of these inserts in enzyme activity have been investigated [69], the specific details of the interaction between the *Pf*AdoMetDC and *Pf*ODC domains and the contributions of the inserts to interdomain protein-protein interactions remain unclear.

The 39-residue O1 insert of *Pf*ODC differs from the other inserts since it is: 1) devoid of low-complexity regions; 2) better conserved between plasmodia in terms of sequence composition and length; and 3) contains an area of well-defined predicted secondary structure [69,121]. These features suggest a distinct function for the O1 insert compared to the other less-conserved and larger inserts in terms of protein folding, stability, organisation and activity [146]. This was confirmed by the observed 94% and 77% reduction in *Pf*ODC and *Pf*AdoMetDC activities, respectively, within the bifunctional complex after deletion of this insert. Moreover, O1 insert deletion prevented *Pf*ODC homodimerisation as well as association with the *Pf*AdoMetDC domain [69], possibly by altering the conformation of *Pf*ODC at the dimer interface. The homology model of monofunctional *Pf*ODC showed that the O1 insert appears to lie parallel to the protein core and loops from the protein surface out towards the C-terminus at the same side as the entrance to the active site [127]. The insert is also flanked by mobile Gly residues (Gly1036-1038 and Gly1083, numbered according to the bifunctional protein) [121] suggesting

that the insert may be acting as a flexible gate-keeping loop for substrate entry into the active site pocket. The O1 insert is thus implicated in both inter- and intradomain protein-protein interactions, mediated by long-range effects across the bifunctional complex and might function as a modulator of interactions between the decarboxylase domains in *Pf*AdoMetDC/ODC. In contrast, the larger O2 insert does not form significant secondary structures and was shown to be more important for *Pf*ODC activity, possibly due to it being spatially removed from the N-terminal *Pf*AdoMetDC domain [69]. However, this insert contains a low-complexity region of (NND)-repeats that are thought to play an important role in the formation of the *Pf*ODC homodimer through the formation of a polar zipper.

The interaction sites between the domains of *Pf*AdoMetDC/ODC therefore remains to be identified while the noteworthy effect that the deletion of the O1 parasite-specific insert has on the entire protein indicates that this insert may be involved in protein-protein interactions across the bifunctional complex. This is based on previous studies that showed the presence of these inserts between structured domains of multiprotein complexes as well as in proteins that have diverse protein binding partners [140]. Analysis of the specific functions of this insert could therefore provide an indication of the arrangement of the domains within the bifunctional *Pf*AdoMetDC/ODC complex. Furthermore, it was postulated that the predicted flexibility of the O1 insert may allow the modulation of the catalytic activity of the *Pf*ODC domain by stabilising the substrate and/or co-factor interactions within the active site pocket, followed by product release. This postulate is substantiated by the homology model of *Pf*ODC in which the O1 insert was shown to be positioned on the same side of substrate entry into the *Pf*ODC active site pocket [135]. Alternatively, the conserved α-helix within the O1 insert may mediate specific protein-protein interactions for *Pf*ODC homodimerisation (intradomain interactions) and/or subsequent complex formation with *Pf*AdoMetDC (interdomain interactions). In this study, mutagenesis, biochemical, computational and peptide probe studies were therefore employed to investigate the possibility that the O1 insert acts as a flexible, catalytically essential loop and to delineate the function(s) of the conserved secondary structure within this insert. The results provide specific evidence for the functional role of the O1 insert in the activities and interdomain associations of *Pf*AdoMetDC/ODC. Furthermore, the role of this insert in protein-protein interactions could in future be used as a platform for the design and application of compounds that could interfere with these interfaces [130].

2.2.Methods

2.2.1. Secondary structure predictions of the O1 parasite-specific insert

The *Odc* gene sequences of *Homo sapiens* (GenBank ID: P11926) and *T. b. gambiense* (Q9TZZ6) as well as the full-length bifunctional plasmodial *Adometdc/Odc* sequences of *P. falciparum* (Q8IJ77), *P. berghei* (Q4YHB2) and *P. yoelii* (Q7RFF2) were subjected to the CLUSTALW2 multiple sequence alignment tool [147] followed by secondary structure predictions with the Jnet v2.0 algorithm within Jpred 3 [148].

2.2.2. Expression constructs and site-directed mutagenesis

The pASK-IBA3 vector (C-terminal Strep-tag, Institut für Bioanalytik, IBA) containing the bifunctional wild-type *PfAdometdc/Odc* coding sequence [70] was used as template for site-directed mutagenesis. The codons encoding the three conserved N-terminal Gly residues (Gly1036-1038, numbering according to bifunctional protein) flanking the O1 insert were mutated to Ala to produce the *A/O G1A* triple mutant. This mutated gene was subsequently used as template to introduce the C-terminal Gly1083Ala mutation resulting in the *A/O G2A* quadruple mutant. The predicted α-helix within O1 was disrupted by the introduction of a Pro codon at residue position 1068 giving rise to the *A/O I1068P* mutant. The primers used for PCR-mediated mutagenesis are listed in Table 2.1.

To create mutations within the monofunctional *Pf*ODC domain, *PfOdc* together with 432 nucleotides of the hinge region, previously cloned into pASK-IBA7 (N-terminal Strep-tag) [103], was used as template with the same primers listed in Table 2.1. Mutagenesis resulted in the monofunctional quadruple *ODC G2A* and helix breaker *ODC I1086P* mutations.

Pfu DNA Polymerases (2.5 U, Fermentas) was used in the presence of 10 fmol template and 10 pmol of each of the primers. Temperature cycling was performed as follows: 94°C for 3 min followed by 30 cycles of 94°C for 30 s, 60°C for 1 min, 68°C for 2 min/kb with a final extension step at 68°C for 10 min. Post-PCR manipulation was performed as described previously [150]. Briefly, the PCR products were visualised with DNA gel electrophoresis and the correctly-sized bands were excised and purified with the NucleoSpin® Extract II PCR cleanup kit (Macherey-Nagel). Purified products were then treated with *Dpn*I (Fermentas) to remove the parental templates for 3 h at 37°C and cleaned as before.

Table 2.1: Mutagenesis primers used for the introduction of point mutations in the O1 parasite-specific insert

Primer	Tm (°C) [a]	Primer Sequence (5' to 3') [b]	Alteration
G1A_F	69	GGATTTAATTTTTATATAATAAATTTAGCAGCAG CATATCCAGGAGGATTAG	Triple N-terminal Gly1036-1038 to Ala inflexibility mutation
G1A_R	69	CTAATCCTCCTGGATATGCTGCTGCTAAATTTATT ATATAAAAATTAAATCC	
G2A_F	68	CATTTCTCAAGACGAAATATGCATACTATAGTTTT GAAAAAATAACATTGG	Single C-terminal Gly1083 to Ala inflexibility mutation
G2A_R	68	CCAATGTTATTTTTTTCAAAACTATAGTATGCATA TTTCGTCTTGAGAAATG	
I1068P_F	67	GTCTTCAAGAAATTAAAAAAGATCCACAAAAATT TCTTAATGAAGAAACATTTCTC	Ile1068 to Pro helix breaker
I1068P_R	67	GAGAAATGTTTCTTCATTAAGAAATTTTTGTGGAT CTTTTTTAATTTCTTGAAGAC	

[a] The Tm's were calculated according to: 69.3+0.41(%GC)-(650/N), where N is the number of nucleotides [149].
[b] Mutations are underlined.

The linear PCR fragments were ligated overnight to form circular plasmids with 3 U of T4 DNA Ligase (Promega) at 22°C. The plasmids as well as a wild-type control (*A/Owt* and *ODCwt*) were electroporated into DH5α cells. The plasmids (monofunctional *ODCwt*, *ODC I1068P*, *ODC G2A* and bifunctional *A/Owt*, *A/O I1068P*, *A/O G2A*) were isolated with the peqGOLD Plasmid Miniprep kit I (Biotechnologie) and all mutations were confirmed with automated nucleotide sequencing using a BigDye® Terminator v3.1 Cycle Sequencing kit (Applied Biosystems) with the ODCseq1 sequencing primer (5'-TATGGAGCTAATGAATATGAATG-3').

2.2.3. Protein expression and isolation

The pASK-IBA3 and -IBA7 plasmids containing the wild-type *PfAdometdc/Odc* and *PfOdc* sequences, respectively, or the various confirmed mutations (above) were transformed into AdoMetDC and ODC deficient *E. coli* EWH331 expression cells kindly provided by Dr. H. Tabor (National Institutes of Health, MD, USA). Proteins were recombinantly expressed and isolated as Strep-tag fusion proteins as described previously [70]. Colonies were inoculated in Luria-Bertani (LB)-ampicillin (50 µg/ml) and incubated at 37°C for 16 h. These cultures were subsequently diluted 1:100 in 1 litre LB-ampicillin medium and incubated at 37°C with agitation until an OD_{600} of 0.5 was reached and protein expression was induced with 200 µg anhydrotetracycline (AHT, IBA). The cultures were incubated for 16 h at 22°C before the cells were harvested. The pelleted cells were diluted in 10 ml wash buffer (100 mM Tris/HCl, pH 8.0, 150 mM NaCl, 1 mM EDTA) per litre of culture. Lysozyme and 0.1 mM phenylmethylsulphonyl fluoride (PMSF, Roche Diagnostics) was added to the suspension and incubated on ice for 30

min. The cells were disrupted with sonication and the soluble proteins were collected in the supernatants after ultracentrifugation was performed at 4°C for 1 h at 100 000*g*. The pellets were discarded while the supernatants were kept for subsequent affinity chromatography.

The Strep-tagged fusion proteins were purified from the total soluble protein extracts using Strep-*Tactin* affinity chromatography (IBA). Each protein extract was loaded at 4°C onto a Chromabond® 15 ml PP column (Macherey-Nagel) containing a 1 cm^3 bed volume of Strep-*Tactin* beads. The beads were subsequently washed three times with 10 ml wash buffer and the bound protein was eluted with 5 ml elution buffer (wash buffer containing 2.5 mM desthiobiotin, IBA) and collected in fractions on ice. Desthiobiotin reversibly competes with binding to the streptavidin and thus releases the Strep-tagged proteins. The beads were regenerated for future use with regeneration buffer (wash buffer containing 1 mM 4-hydroxy azobenzene-2-carboxylic acid, Sigma-Aldrich), which in turn displaces the desthiobiotin from the affinity beads. Protein concentration was determined by the Bradford assay [150] and visualised with denaturing SDS-PAGE and silver staining [151].The protein samples were kept at 4°C until further use.

2.2.4. Activity analysis of the recombinantly expressed proteins

AdoMetDC and ODC activities were measured by trapping released $^{14}CO_2$ from *S*-[carboxy-^{14}C]adenosyl-L-methionine (60.7 mCi/mmol, Amersham Biosciences) and L-[1-^{14}C]ornithine (55 mCi/mmol, Amersham Biosciences) as previously described [70]. Briefly, 5 µg of the bifunctional or monofunctional proteins were incubated in AdoMetDC (50 mM KH_2PO_4, pH 7.5, 1 mM EDTA, 1 mM DTT) or ODC (50 mM Tris/HCl, pH 7.5, 40 µM PLP, 1 mM EDTA, 1 mM DTT) assay buffers in a total reaction volume of 250 µl containing 100 µM total substrate. The reactions were incubated at 37°C for 30 min followed by reaction termination via protein precipitation with the addition of 0.5 ml of 30% (v/v) trichloroacetic acid. $^{14}CO_2$ was captured with hydroxide of hyamine-treated filter papers (PE Applied Biosystems, USA) for an additional 30 min at 37°C. The filter papers were transferred to 4 ml Pony-Vial H/I tubes (PE Applied Biosystems) to which 4 ml of Ultima Gold XR scintillation fluid (PE Applied Biosystems) was added. The radioactivity was counted with a Tri-Carb series 2800 TR liquid scintillation counter (PE Applied Biosystems). Specific enzyme activity was expressed as the amount of CO_2 produced in nmol/min/mg and performed in duplicate for three individual experiments. The specific activities of the mutant proteins were normalised against the specific activity of the wild-type protein performed in parallel. Statistical analysis was performed using paired Students t-test.

2.2.5. Analysis of the oligomeric status of the mutant monofunctional and bifunctional proteins

The ability of the wild-type and O1 insert mutated proteins to form either monofunctional *Pf*ODC homodimeric (~170 kDa) or bifunctional *Pf*AdoMetDC/ODC heterotetrameric (~330 kDa) proteins [69,70] via protein-protein interactions were determined by size-exclusion chromatography (SEC) using an Äkta Prime System (Amersham Pharmacia Biotech). A Superdex®-S200 10/300 GL SE column (Tricorn, GE Healthcare) was calibrated with the Gel Filtration Standard kit (BioRad), which separated into five peaks corresponding to thyroglobulin (670 kDa), γ-globulin (158 kDa), ovalbumin (44 kDa), myoglobin (17 kDa) and Vitamin B_{12} (1.35 kDa). A standard curve obtained from the elution of the standard proteins was used to identify the fractions in which the monofunctional *Pf*ODC homodimeric (~170 kDa) or monomeric (~85 kDa) and bifunctional *Pf*AdoMetDC/ODC heterotetrameric (~330 kDa) or heterodimeric (~165 kDa) proteins were expected to elute. The column was equilibrated with wash buffer and equal amounts of separately expressed and isolated monofunctional *Pf*ODC (ODCwt, ODC I1068P and ODC G2A) and bifunctional *Pf*AdoMetDC/ODC (A/Owt, A/O I1068P and A/O G2A) proteins (~120 µg) were each applied to the SEC column and 1.5 ml fractions were collected at a flow rate of 0.5 ml/min in wash buffer.

2.2.6. Western immunodetection of monofunctional *Pf*ODC and bifunctional *Pf*AdoMetDC/ODC proteins following SEC

The *Pf*AdoMetDC/ODC and *Pf*ODC proteins were detected in each fraction with dot-blot Western immunodetection. Briefly, 0.5 ml of the sequential fractions collected from SEC were dot-blotted onto Immobilon-P PVDF transfer membranes (Millipore) using a BioDot apparatus (Bio-Rad). The membranes were subsequently blocked for 16 h at 4°C with blocking buffer (1xPBS containing 3% (w/v) BSA, 0.5% (v/v) Tween-20). For immunodetection of the Strep-tag fusion protein the membranes were incubated for 1 h at 37°C in membrane wash buffer (1xPBS containing 1% BSA, 0.5% Tween-20) and 1:4000 monoclonal Strep-tag II horseradish peroxidase (HRP)-conjugated mouse antiserum (Acris antibodies). The antibody is coupled to keyhole limpet haemocyanin and is supplied as a liquid Protein G purified immunoglobin fraction, conjugated to HRP and therefore does not require the incubation with a secondary antibody. The membranes were washed six times in the membrane wash buffer followed by incubation for 5 min in equal volumes of the Luminol/Enhancer and Stable Peroxidase solutions (SuperSignal® West Pico Chemiluminescent Substrate, Pierce). Hyperfilm High Performance chemiluminescence films (Amersham Biosciences) were exposed for various times to the membranes and subsequently developed (3 min) and fixed (1 min) with ILFORD Universal

Paper Developer and Rapid Fixer, respectively (ILFORD Imaging Ltd., UK). Images of the developed film were captured with a VersaDoc™ Imaging System (BioRad).

2.2.7. Computational studies on the homology models of the monofunctional *Pf*AdoMetDC and *Pf*ODC proteins

The following *in silico* simulations were performed by G. A. Wells [152] to visualise the flexibility of the O1 insert and the subsequent role of the flanking Gly residues on this flexibility upon their mutagenesis to Ala. Briefly, homology models for both AdoMetDC and ODC domains were constructed for all full-length *Plasmodium* spp listed in PlasmoDB (*P. falciparum*, *P. vivax*, *P. knowlesi*, *P. yoelii* and *P. berghei*) [3]. The monomeric AdoMetDC domain was modelled with the human (1I7B) and *S. tuberosum* (1MHM) as templates, while the homology model of dimeric ODC was optimised from earlier models [127] using MODELLER 9v2. Model qualities were determined using PROCHECK [153] and WHATIF [154].

For molecular dynamics (MD) simulations of *P. falciparum* ODC, 30 models were constructed with the O1 insert included. Based on the secondary structure predictions, the backbone conformation of residues 1054-1060, 1061-1072 and 1074-1076 of the O1 insert were restricted to a β-strand, α-helix and α-helix, respectively. A model of the A/O G2A mutant was constructed in VMD [155] using the wild-type structure as template. MD was performed on the wild-type and A/O G2A models using NAMD 2.6 [156].

For protein-protein docking, multiple (~100) models were constructed for the AdoMetDC and ODC domains, including an average or cluster model. All parasite-specific inserts were excluded from modelling to avoid additional uncertainty. Wild-type AdoMetDC models were docked against wild-type dimeric ODC models using FTDOCK2 [157] with AdoMetDC being treated as the mobile species while ODC was kept static.

2.2.8. Incubation of *Pf*AdoMetDC/ODC with synthetic peptide probes

Synthetic peptides were designed to specifically target and compete with the inter- and intradomain interacting sites of the O1 insert: 1) NY-39 is identical to the entire O1 insert and is expected to bind to the insert's interaction site; 2) LK-21 is identical to the α-helix within the O1 insert and would thus also bind to the α-helix interaction site; while 3) LE-21, was designed as the charge complement of the helix within the O1 insert by replacing the positively-charged Lys with negatively-charged Glu residues in the peptide and *vice versa* to enable binding to the helix

(Table 2.2). The peptides were synthesised and purified to >95% purity (GL Biochem Ltd., China). The wild-type *Pf*AdoMetDC/ODC protein was purified as above and incubated with the peptides at 10-, 100- and 1000-fold molar excess of the peptides at 22°C for 2 h with moderate agitation. The peptide-treated samples were subsequently subjected to AdoMetDC and ODC activity assays as described previously [70]. The activity of the untreated, wild-type *Pf*AdoMetDC/ODC protein was used as a positive control to give an indication of the extent to which the peptide affected the bifunctional protein's activity. The activities of the samples, obtained from three independent experiments performed in duplicate, were normalised to the activity of the positive control and expressed as a percentage of this activity. The results were compared using a directional one-tailed Student t-Test assuming unequal variances.

2.3. Results

2.3.1. The O1 parasite-specific insert contains specific structural features

In-depth secondary structure predictions were performed on the O1 inserts from three different *Plasmodium* spp (*P. falciparum*, *P. berghei* and *P. yoelii*) using the Jnet algorithm v2.0, which provides a prediction of secondary structures with an accuracy of 81.5% [148]. The *P. falciparum*-specific O1 insert (residues 1047-1085) is flanked by three plasmodia-conserved N-terminal Gly residues [69] and a single non-conserved C-terminal Gly residue located within the insert (Figure 2.1). These Gly residues could contribute to insert flexibility due to the many bond rotational conformations Gly residues can assume [158]. Moreover, the predictions showed that the 39-residue O1 insert does have a propensity to form a plasmodia-conserved α-helix (Figure 2.1) [121]. Subsequent experiments investigated the possible roles of the flexibility as well as the presence of a predicted secondary structure within the O1 insert.

Figure 2.1: Multiple sequence alignment and secondary structure prediction of the O1 insert. Plasmodial sequences of *P. falciparum* (PFAM, GenBank ID: Q8IJ77), *P. yoelli* (PYOEL, Q7RFF2) and *P. berghei* (PBERGH, Q4YHB2) were used and the corresponding ODC sequences of *H. sapiens* (HUMAN, P11926) and *T. b. gambiense* (TRYBG, Q9TZZ6) are also shown. Similar and identical residues are shown in light and dark blue, respectively. The conserved N-terminal Gly1036-1038 residues and non-conserved C-terminal Gly1083 of *Pf*ODC are indicated by boxes and the Ile1068 residue that was mutated to a Pro is shown with a red box. Dashed lines are areas where the O1 inserts are absent in the HUMAN and TRYBG sequences. The predicted *Pf*ODC β-sheets (green arrows) and conserved α-helix (red cylinder) are shown below the alignment.

2.3.2. Mutagenesis of the flanking Gly residues and disruption of the α-helix within O1 insert affects enzyme activity

To test the hypothesis that the Gly residues flanking the O1 insert provide loop flexibility and are involved in the decarboxylase activities of *Pf*AdoMetDC/ODC, the N- and C-terminal O1 insert Gly residues were replaced with Ala. This resulted in a triple mutant A/O G1A (Gly1036-1038 to Ala) protein where only the flanking N-terminal Gly residues were mutated, and a quadruple A/O G2A mutant (Gly1036-1038 and Gly1083 to Ala) where both the N- and C-terminal Gly residues were mutated. Secondly, to investigate the possible role of the conserved O1 insert α-helix in the decarboxylase activities of the bifunctional *Pf*AdoMetDC/ODC enzyme by mediating inter- and intradomain protein-protein interactions, a helix-breaker Pro residue was inserted within this helix resulting in the A/O I1068P mutant protein. The secondary structure prediction of this mutant using the Jnet algorithm did not predict the presence of an α-helix (results not shown).

Compared to the wild-type enzyme, the specific activity of the *Pf*AdoMetDC domain in the bifunctional protein was significantly (P<0.01) reduced by 83% and 67% in the triple (A/O G1A) and quadruple (A/O G2A) mutant enzymes, respectively. In addition, the *Pf*ODC domain in both Gly mutant enzymes were essentially inactivated (P<0.01) (Figure 2.2).

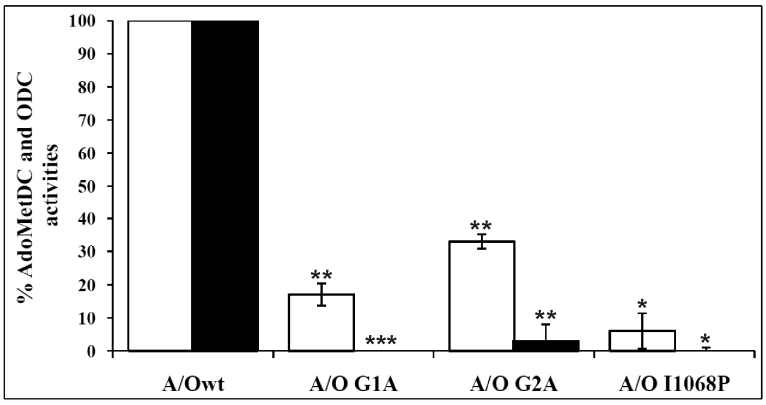

Figure 2.2: The effect of O1 insert mutations on the *Pf*AdoMetDC and *Pf*ODC enzyme activities within the bifunctional complex.
The AdoMetDC (white bars) and ODC (black bars) specific activities of the mutant enzymes (A/O I1068P, A/O G1A and A/O G2A) were normalised to the wild-type activity (A/Owt) and are given as a percentage. The results are shown as mean ± S.E.M with error bars on each graph from three independent experiments carried out in duplicate (n=3). Significant differences at a confidence level of 95% are represented as follows: * for P<0.05; ** for P<0.01; *** for P<0.001.

Disruption of the O1 insert α-helix (A/O I1068P) also resulted in complete loss in *Pf*ODC specific activity and significantly decreased *Pf*AdoMetDC activity (P<0.05) (Figure 2.2). It is therefore possible that the helix within the O1 insert is involved in protein-protein interactions

with both domains of the bifunctional complex and that the flexibility of the insert may allow these interactions to take place. Disruption of the helix may therefore be communicated to the respective sites via long-range interactions [134] resulting in the reduced activities of both domains. Alternatively, mutagenesis may hinder substrate binding to the *Pf*ODC active site due to its proximate location to the active site entrance [127]. However, increased substrate concentrations of up to 400 µM (8-fold K_m) did not restore AdoMetDC or ODC activity for any of the mutant enzymes, which indicates that altered K_m's were not responsible for the loss of enzyme activities (results not shown). The results therefore show that the flexibility of the O1 insert (imparted by the flanking Gly residues), as well as the α-helix within this insert are functionally important for both the *Pf*AdoMetDC and *Pf*ODC domains.

2.3.3. The O1 insert α-helix mediates inter- and intradomain protein-protein interactions

SEC on affinity-purified wild-type and mutated monofunctional and bifunctional proteins was performed to qualitatively determine if loss of catalytic activity could be ascribed to the inability of the mutant proteins to form obligate *Pf*ODC homodimers and to associate into bifunctional *Pf*AdoMetDC/ODC complexes. Interestingly, even though equal amounts of total protein were applied to SEC, the quantities of proteins in specific fractions of the mutated protein samples were decreased for both the mutant bifunctional *Pf*AdoMetDC/ODC and monofunctional *Pf*ODC protein preparations. These differences in protein levels between the wild-type and the mutant samples were also detected with SDS-PAGE analysis (results not shown) and are probably due to the formation of larger, soluble protein aggregates upon mutagenesis.

The expected sizes of the wild-type heterotetrameric *Pf*AdoMetDC/ODC protein (A/Owt) and its heterodimeric form are shown in Figure 2.3A. *Pf*ODC was also expressed in its monofunctional form resulting in a homodimeric protein (with half of the hinge region) with a size of ~170 kDa, due to the association of two ~85 kDa monomeric proteins (Figure 2.3B) [103]. Prevention of heterotetrameric complex formation or dimerisation of the *Pf*ODC domains as a result of the introduced mutations would therefore be reflected in the SEC profiles. As expected, the wild-type bifunctional A/Owt protein eluted as both heterotetrameric (~330 kDa, fractions 44-46 of the SEC) and heterodimeric (~165 kDa, fractions 53-55) proteins (Figure 2.3A) due to the equilibration between bound and unbound states of the *Pf*ODC domains in the bifunctional protein [23]. Moreover, disruption of the α-helix in the O1 insert prevented not only heterotetramer complex formation but also dimerisation of the *Pf*ODC domain, which is obligatory for activity [127]. This is evident for both the bifunctional A/O I1068P protein that

eluted as a heterodimer of ~165 kDa (Figure 2.3A) as well as the monofunctional ODC I1068P protein that eluted as a monomer of ~85 kDa (Figure 2.3B). These results support previous findings, which have shown that dimeric *Pf*ODC is a prerequisite for heterotetrameric complex formation [69].

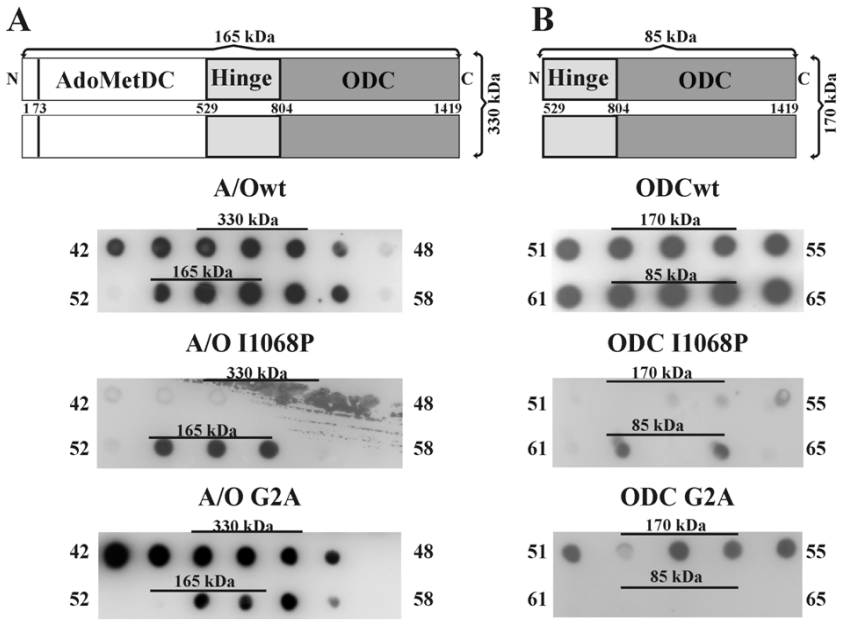

Figure 2.3: Western blots of the sequential fractions obtained from SEC of the (A) bifunctional *Pf*AdoMetDC/ODC and (B) monofunctional *Pf*ODC proteins.
From the top to the bottom panel the blots are shown for the wild-type (wt), the α-helix disrupted (I1068P) and the immobile (G2A: Gly1036-1038, 1083 to Ala) proteins. The sizes of the proteins in the SEC fractions as determined from a standard curve are indicated with black bars. Schematic diagrams to show the predicted sizes of the bifunctional *Pf*AdoMetDC/ODC (~330 or ~165 kDa) and monofunctional *Pf*ODC (~170 or ~85 kDa) proteins are shown above the blots.

These results also show that the protein-protein interactions that are required for complex formation are independent of the proposed flexibility of the O1 insert since SEC showed that the inflexible and inactive A/O G2A mutant could still form the ~330 kDa heterotetrameric complex (Figure 2.3A, fractions 44-46). Furthermore, while the equilibration of the bound and unbound states of wild-type *Pf*ODC was maintained (Figure 2.3B), the Gly mutations shifted the equilibrium towards the formation of the inactive ~170 kDa *Pf*ODC homodimer (Figure 2.3B, fractions 52-54). It therefore seems that the Gly residues are more important for the O1 insert's involvement in the decarboxylase activities of *Pf*AdoMetDC/ODC (Figure 2.2) than in complex formation.

Since the Gly to Ala mutations in the A/O G2A did not influence dimerisation, the loss of activity for this mutant may therefore be ascribed to a loss of insert flexibility. Therefore, to localise the O1 insert and to show the inflexibility of the quadruple Gly mutant, MD simulations were preformed (Figure 2.4). MD can be used to simulate the movement of the insert and

thereby provide information on the effect of the flanking Gly residues on the insert movement, which would not be possible in laboratory experiments.

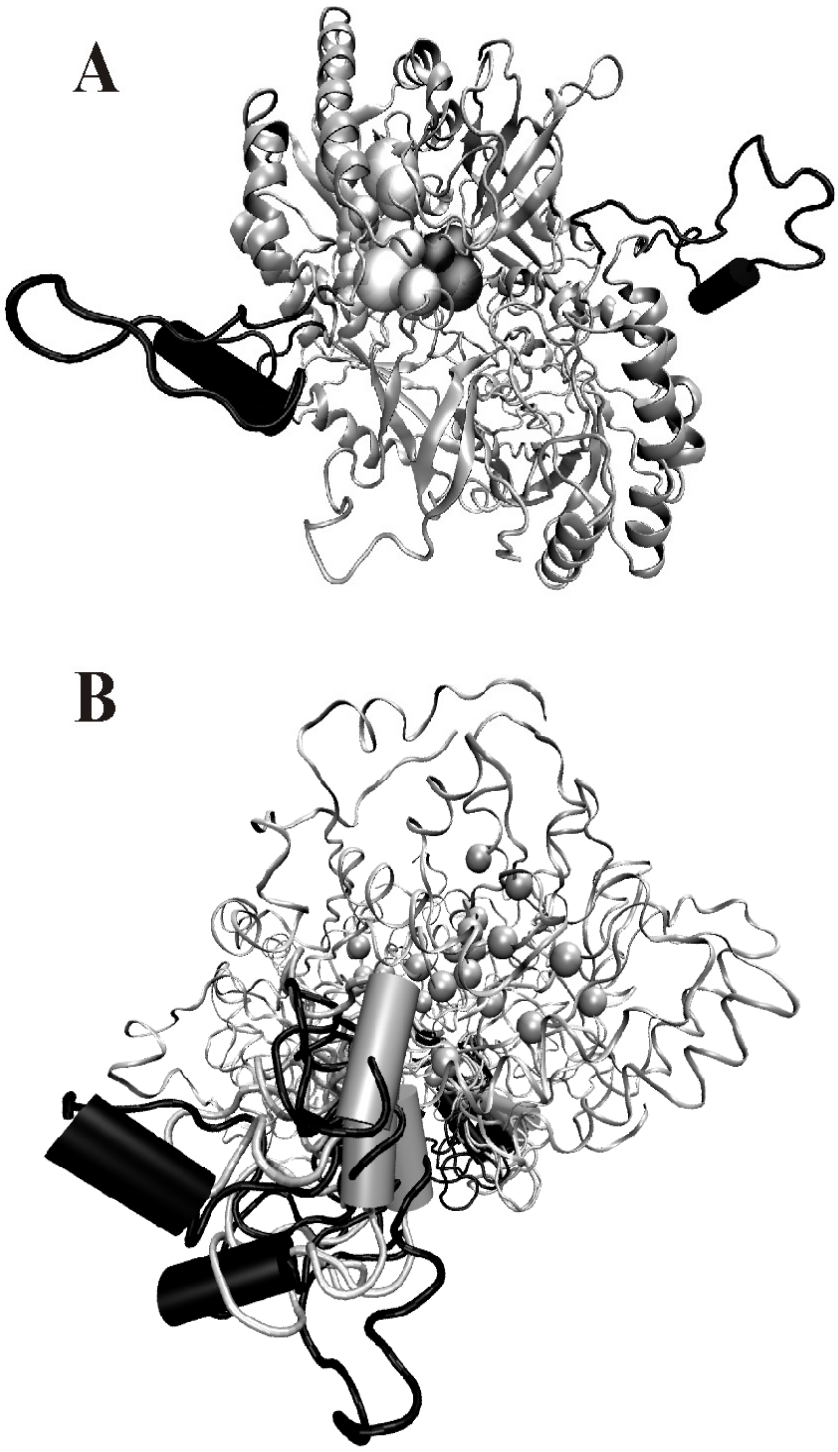

Figure 2.4: The wild-type homodimeric *Pf*ODC and immobile insert ODC G2A mutant protein after minimisation and MD.
(A) To give an indication of the protein and insert arrangement prior to MD, the two monomers of the wild-type *Pf*ODC minus its O1 inserts, prior to 5 million dynamic steps are shown in grey while only the O1 inserts of the ODC G2A mutant are shown in black relative to the active site (grey spheres). (B) A side view of the protein with the inserts (wild-type and mutant inserts shown in grey and black, respectively) at the front and back of the page after MD. The *Pf*ODC active sites and interface residues of the wild-type protein are shown as spheres while the α-helices within the inserts are shown as cylinders.

The results showed that, compared to the mutant insert at the start of the simulation (Figure 2.4A), the O1 insert of the wild-type *Pf*ODC protein appeared more tightly folded against the monomeric *Pf*ODC subunit at the site of substrate entry into the active site pocket (Figure 2.4B) [135]. The insert of the mutant protein projects away from the protein where it is unlikely to interact with the protein core. Interestingly, the α-helix within the O1 insert of the wild-type protein also moves closer to the protein to allow for possible interactions or to stabilise co-factor or substrate binding whereas the α-helix in the ODC G2A mutant protein remains more distant from the protein.

Experimental evidence therefore suggests the involvement of the O1 parasite-specific insert and specifically its predicted α-helix, in the functioning and dimerisation of the bifunctional *Pf*AdoMetDC/ODC protein. However, deletion or disruption of the O1 insert as well as mutations of *Pf*AdoMetDC/ODC and *Pf*ODC can have unpredictable effects on protein conformation, which may be communicated through long-range interactions to active site centres and protein-protein interaction sites. In addition, the appearance of soluble aggregates upon mutagenesis could also have an effect on the activities of the protein samples. Peptides were therefore used as novel probes to further aid the interpretation of the mutagenesis results.

2.3.4. Peptide probe-mediated modulation of *Pf*AdoMetDC and *Pf*ODC activities via interference of the O1 insert interactions

Various peptides were designed to be used either as competitors to simulate the functions of the O1 insert i.e. NY-39, which is identical to the entire O1 insert and LK-21, which is identical to the predicted α-helix within insert O1. In addition, a peptide was also designed as a blocking probe to prevent insert-mediated inter- and intradomain interactions (LE-21, a charge complement peptide of the predicted α-helix within insert O1) (Table 2.2).

Table 2.2: The synthetic peptides used as probes to determine the role of the O1 insert in protein-protein interactions across *Pf*AdoMetDC/ODC

Peptide	Peptide sequence [a]
NY-39	NAKKHDKIHYCTLSLQEIKKDIQKFLNEETFLKTKYGYY
LK-21	LSLQEIKKDIQKFLNEETFLK
LE-21	LSLQ***KIEE***DIQ***E***FLQ***KK***TFL***E***

[a] The common sequences that are predicted to form the α-helix within insert O1 are underlined. The charge complement residues in peptide LE-21 are shown in bold italics.

Treatment of *Pf*AdoMetDC/ODC with the peptides significantly increased (P<0.05) *Pf*AdoMetDC activity by ~60% at the highest concentrations tested (Figure 2.5A) by presumably

interacting with the respective target sites of these peptides within the *Pf*AdoMetDC and/or *Pf*ODC domains. Peptide NY-39 (corresponding to the complete O1 insert) also significantly increased ($P<0.05$) both *Pf*AdoMetDC and *Pf*ODC activities (Figure 2.5). It can be speculated that the increase in activity could be due to stabilisation of the *Pf*ODC protein-protein interactions that are mediated by the O1 insert. However, the effect of this insert on *Pf*ODC dimerisation was not investigated due to the large quantities of the peptide that are required to determine the oligomeric status of the protein:peptide complex with SEC. In contrast, the α-helix insert peptide (LK-21) increased both domain activities within the bifunctional *Pf*AdoMetDC/ODC in an almost dose-dependent manner but only the highest peptide concentration significantly ($P<0.05$) affected *Pf*AdoMetDC and *Pf*ODC activities (Figure 2.5A and B). The results show that the NY-39 peptide has additional effects beyond the proposed O1 insert α-helix effects on both domains due to the significant increases in both domain activities at all concentrations tested.

The O1 insert charge complement peptide LE-21, significantly decreased *Pf*ODC activity by 43% ($P<0.05$) at a 1000-fold molar excess of the peptide (Figure 2.5B). This peptide possibly interferes with beneficial inter- and/or intradomain protein-protein interactions that are normally mediated by the O1 insert. One consequence could be prevention of *Pf*ODC homodimer formation, which is translated to inhibition of the interaction of this domain with the *Pf*AdoMetDC domain, but this was not determined due to the limited quantities of the peptide that was available.

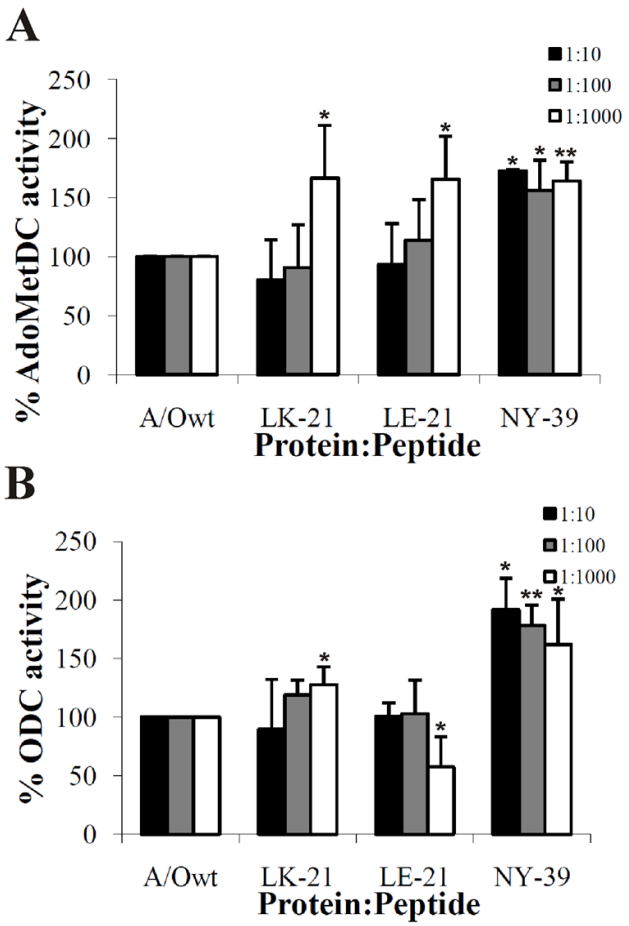

Figure 2.5: *Pf*AdoMetDC (A) and *Pf*ODC (B) activities after co-incubation with different peptide probes. The specific activities (nmol/min/mg) of the peptide-treated enzymes were normalised to the untreated, positive control's activity (A/Owt) and are given as a percentage. The values were determined from three independent experiments carried out in duplicate (n=3) after a 2 h incubation at 22°C of the wild-type bifunctional protein with three different peptides at three different molar quantities (protein to peptide ratio in molar quantities of 1:10, 1:100, 1:1000). The standard deviations of the mean are indicated as error bars on each graph. Significant differences at a confidence level of 95% are represented as follows: * for $P<0.05$ and ** for $P<0.01$.

From these results it is plausible that the O1 insert forms direct interactions with both domains in the bifunctional protein to modulate the decarboxylase activities. The peptides (LK-21 and NY-39) behave as O1 insert mimics and simulate inter- and intradomain protein-protein interactions of the O1 insert as reflected by the increases in *Pf*AdoMetDC and *Pf*ODC activities. The LE-21 charge complement peptide increases *Pf*AdoMetDC activity to the same extent as LK-21 but inhibited the activity of the *Pf*ODC domain by blocking the interactions normally mediated by the α-helix within the O1 insert (Figure 2.5A and B). Non-specific stabilisation and inhibitory effects of peptide binding seem unlikely since specific up- and down-regulation of the enzymatic activities were observed and the increase in peptide concentrations affected the enzyme activities in a dose-dependent manner. Furthermore, in the absence of CD analysis, the peptides in solution are predicted to fold into α-helices as determined by PEP-FOLD (Figure 2.6) [159]. The folding of the peptides into their 3D shapes is expected to allow the peptides to form interactions with their predicted target sites.

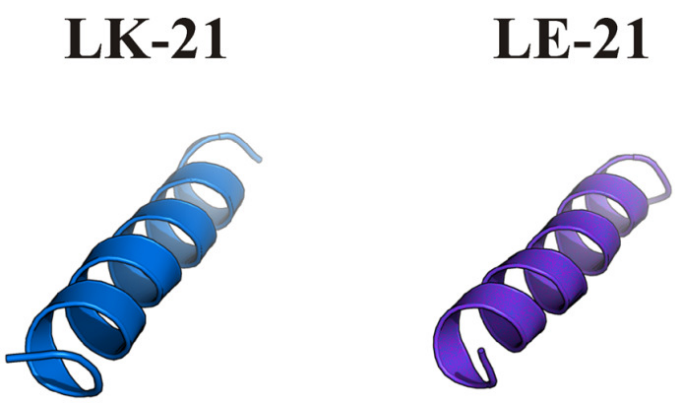

Figure 2.6: Folding of the α-helix O1 insert peptides as predicted by PEP-FOLD.

To determine whether the α-helix within the O1 insert of the *Pf*ODC domain is positioned in such a way that it is capable of forming direct interactions with the *Pf*AdoMetDC protein, protein-protein docking was employed to monitor the interaction between *Pf*AdoMetDC and *Pf*ODC. Even though the parasite-specific inserts were removed from these models prior to docking, their approximate positions on the *Pf*ODC protein could still be established (Figure 2.7).

In general, the docking results predicted that *Pf*AdoMetDC only makes contact with one face of the *Pf*ODC homodimeric protein, which is the same region where the *Pf*ODC active site and the O1 insert are located [152]. Fewer contacts are predicted for the non-active site face (Figure 2.7). Conversely, only one face of *Pf*AdoMetDC is favoured for contact with *Pf*ODC (results not shown) [152]. By taking into consideration the volume that would be occupied by the *Pf*AdoMetDC protein (identified as spheres in Figure 2.7) it is conceivable that the O1 insert (identified by the positions of the red spheres) is positioned in such a way that an interaction between the insert and the *Pf*AdoMetDC domain would be allowed. The same result was observed for AdoMetDC and ODC proteins from the five plasmodial species that were modelled, which indicates that the mechanism of protein-protein interactions between the domains is preserved and emphasises the importance of the conserved O1 parasite-specific insert in possibly mediating these essential inter- and intradomain interactions that are required for optimal enzyme activities within the bifunctional *Pf*AdoMetDC/ODC.

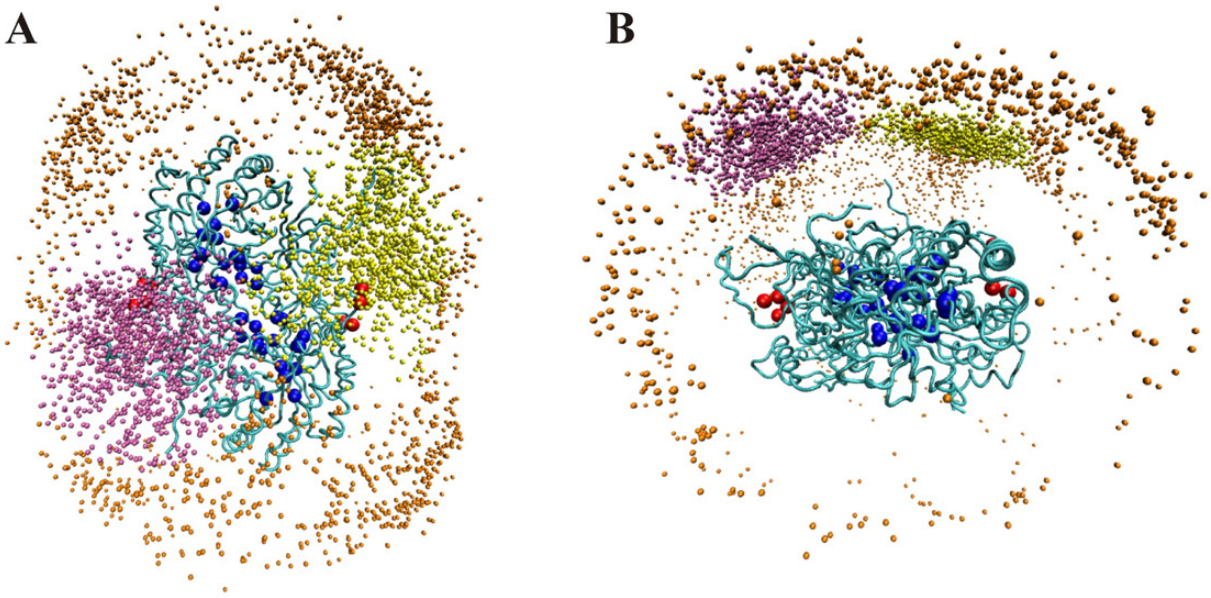

Figure 2.7: Protein-protein docking results to determine the proximity of the O1 insert to the *Pf*AdoMetDC protein.
(A) The view from the bottom of the ODC dimer at the site of substrate entry into the active site pockets and (B) a side view of the protein with the ODC actives sites at the top. The orange, yellow and magenta spheres represent the centre of mass of different AdoMetDCs around the homodimeric ODC protein (blue ribbon). These spheres are the favoured positions of the AdoMetDCs, which are approximately symmetrical. The entire inserts were not included in the model but the positions of the O1 inserts can be identified by the red spheres. The ODC active site residues at the homodimer interface are shown as blue spheres (numbered according to the bifunctional protein): Chain A: Lys868, Asp887, Glu893, Arg955, His998, Ser1001, Asn1034, Gly1037, Glu1114, Gly1116, Arg1117, Asp1320, Tyr1384; Chain B: Tyr1311, Asp1356, Phe1392, Asn1393, Phe1395.

2.4.Discussion

Investigations into the roles of the hinge region connecting the *Pf*AdoMetDC and *Pf*ODC domains as well as parasite-specific inserts within both domains showed that the *Pf*ODC domain is more refractory to interference and possibly acts as the nucleation site for the formation of the active bifunctional complex in *P. falciparum* [69,103]. Such interdomain associations have also been observed for *P. falciparum* DHFR/TS, in which the catalytic activities of DHFR and TS are increased when the adjacent domain is in its activated, ligand-bound conformation [160]. *P. falciparum* TS is also dependent on its physical interaction with the DHFR domain for catalytic activity and possible allosteric regulation [122]. Furthermore, a crossover helix within a non-active site region of *Cryptosporidium hominis* DHFR has been shown to physically interact with the active site of the other DHFR monomer, thereby modulating its activity [161].

In the absence of known regulatory mechanisms of both *Pf*AdoMetDC and *Pf*ODC, the arrangement of the proteins within the bifunctional complex has been proposed to allow for the regulation of the enzyme activities via protein-protein interactions as has been observed in other

organisms. Mammalian ODC is rapidly degraded by its association with an inhibitory, polyamine-dependent antizyme protein [162] and the efficiency of the catalytic activity of trypanosomal AdoMetDC is dependent on its association with a catalytically dead, but allosterically active, AdoMetDC homologue or prozyme [163,164]. However, in *P. falciparum*, while antizyme is absent and the presence of a prozyme seems improbable, *Pf*AdoMetDC/ODC may behave in an analogous fashion to the DHFR/TS association where the enzyme properties are co-regulated to control polyamine biosynthesis.

Previous studies showed depletion of *Pf*ODC activity upon the deletion of the O1 parasite-specific insert from the bifunctional *Pf*AdoMetDC/ODC protein as a result of the inability to form active *Pf*ODC homodimers [69]. Two possible roles for the O1 insert were therefore investigated in this study. The first hypothesis, which is supported by a *Pf*ODC homology model [127], implies that the position and the proposed flexibility imparted by the flanking Gly residues of the O1 insert allows it to function as a catalytically essential loop. Secondly, it was postulated that the position of the O1 insert on the surface of the protein could allow the insert to mediate essential inter- and intradomain protein-protein interactions.

Flexible active site loops have been described for the Lys169 trypsin-sensitive loops of *L. donovani* [165] and *T. brucei* ODC [134] as well as for *Pf*ODC [127], where they retain the substrate within the active site pocket for catalysis and then open to allow the release of product. In addition to this trypsin-sensitive flexible loop, the O1 insert of *Pf*ODC is also sensitive to trypsin digestion, which suggests that it is located on the surface of the protein and exposed to the solvent [166]. This insert may additionally enable the stabilisation of the PLP co-factor within the *Pf*ODC active site as predicted by the *Pf*ODC homology model [127]. Similarly, the PLP-dependent *E. coli* D-serine dehydratase contains a flexible Gly-rich region that interacts with the co-factor [167]. For the *T. brucei* ODC enzyme, the presence of a highly flexible and conserved Gly-rich region (Gly235-237, corresponding to Gly1036-1038 in *Pf*ODC) and a salt bridge to Arg277 (corresponding to Arg1117 in *Pf*ODC) was shown to stabilise binding of PLP within the active site [168]. In this study, it was shown that the proposed restriction of O1 insert flexibility through mutation of the flanking Gly residues to Ala resulted in a loss of the specific activities of both domains of the bifunctional *Pf*AdoMetDC/ODC complex (Figure 2.2). The N-terminal Gly residues (Gly1036-1038) are also conserved within plasmodial ODCs and could thus serve as a binding site for PLP, which would explain the depletion of the specific activities of both the triple and quadruple mutants (A/O G1A and G2A). The observed decrease in

*Pf*AdoMetDC activity could be due to long-range effects communicated to this domain's active site upon inactivation of the *Pf*ODC domain. Enzyme kinetics to determine whether PLP binding to *Pf*ODC was affected was not performed due to the inactivation of the enzymes upon mutagenesis. On the other hand, the C-terminal Gly residue of the O1 insert (Gly1083) is not conserved among plasmodial ODCs (Figure 2.1) and is not predicted to play a role in the activity of *Pf*ODC activity. It therefore seems that the mutagenesis of the Gly residues resulting in inactive enzymes were due to prevention of co-factor binding and not as a result of insert inflexibility.

SEC of the G2A mutant protein showed that the protein was still capable of forming the homodimeric *Pf*ODC domain. However, disruption of the α-helix within the O1 insert through the introduction of a Pro residue showed that this I1068P mutant could no longer form the obligate *Pf*ODC homodimer (Figure 2.3). Additionally, this mutation prevented the formation of the bifunctional heterotetrameric *Pf*AdoMetDC/ODC complex, which resulted in significant losses in both enzyme activities (Figure 2.2). This result emphasises the importance of *Pf*ODC homodimer formation as nucleation sites for heterotetrameric bifunctional complex association [69].

Previous studies have shown that monofunctional *Pf*AdoMetDC has an increased substrate affinity when associated with *Pf*ODC in the bifunctional *Pf*AdoMetDC/ODC complex [71]. The identification of the interaction sites that mediate the interdomain interactions would therefore provide interesting opportunities to simultaneously influence both decarboxylase domains of the bifunctional complex. In this study, the disruption of the conserved α-helix within the O1 insert significantly decreased both *Pf*AdoMetDC and *Pf*ODC activities within the bifunctional complex but also prevented complex formation. This helix thus represents a site that can be targeted for the simultaneous interference of the activities of the bifunctional *Pf*AdoMetDC/ODC. Additionally, protein-protein docking results confirmed that the O1 insert (and possibly the α-helix within this insert) is in close enough proximity to the active site faces of *Pf*AdoMetDC to enable physical interactions with the protein (Figure 2.7).

The possibility that the O1 insert acts as a key enzymatic regulator of decarboxylase activity within the bifunctional complex was further investigated with novel peptides as probes in an attempt to distinguish between the effects of global conformational changes introduced as a result of the mutations as opposed to the effects of more localised interventions. Synthetic

peptides have been successfully applied as inhibitors of *P. falciparum* TIM [169], HIV-1 protease [170,171], *Lactobacillus casei* TS [172] and *T. brucei* farnesyltransferase [173]. For *Pf*TIM, one peptide resulted in a 55% decrease in enzyme activity at a 1000-fold molar excess of the peptide, which indicated that this region is possibly involved in the stabilisation of the dimeric protein [169]. However, the use of peptides to probe interaction sites of a specific protein region in order to obtain information on the structural arrangement of a protein represents a novel application of synthetic probes in biochemistry.

Analysis of the residues within the O1 insert within *Pf*ODC revealed the presence of two dominant motifs: a cationic N-terminal motif (high abundance of Lys residues) and an aromatic C-terminal motif (high abundance of aromatic residues) (Table 2.2). These may be involved in different interactions with the core protein such as electrostatic interactions/hydrogen bonds and aromatic stacking/hydrophobic interactions, respectively. Therefore, synthetic peptides were specifically designed based on these areas to probe the functional roles of the O1 insert.

The NY-39 peptide, which mimics the entire O1 insert and thus contains both the N-terminal cationic and C-terminal aromatic motifs, is expected to compete for binding to the native sites of the insert on *Pf*ODC (intradomain interactions) and/or *Pf*AdoMetDC (interdomain interactions). The significant increase by the peptide in the specific activities of both enzymes after treatment with this peptide suggests relief of restraints imposed on the domains through interactions that are natively mediated by the O1 insert. The role of the peptide in mediating complex formation could not be determined but would provide additional information on the role of the insert in mediating complex formation as was observed with the SEC results of the α-helix mutant. These effects were less pronounced when the shorter peptide LK-21 was used.

The LK-21 peptide is identical to the α-helix within O1 and was also expected to compete with the native interaction sites of specifically the α-helix within the O1 insert as the NK-39 peptide would. Treatment of the bifunctional protein with this peptide resulted in a dose-dependent increase of the specific activities of both *Pf*AdoMetDC and *Pf*ODC, which was less pronounced in *Pf*ODC activity. Subsequently, and to gain a better understanding of the function of the α-helix, the effects of a charge complementary peptide of the helix on *Pf*AdoMetDC/ODC activity were investigated. This mostly anionic peptide is expected to bind to the cationic motif of the O1 insert helix and not to the helices' interaction sites. Whereas the increase in *Pf*AdoMetDC activities by this peptide was indistinguishable from those of the other peptides, the activity of

the *Pf*ODC domain significantly decreased in a dose-dependent manner. The results therefore suggest that this peptide could form stable ionic interactions with the α-helix in the O1 insert. Peptide binding to the insert then resulted in either the prevention of obligate *Pf*ODC homodimer formation, which decreased its activity and/or prevented the native functioning of the loop in intradomain interactions.

It is feasible that an increase in the proportions of *Pf*AdoMetDC-peptide complexes (peptides LK-21 and NY-39) relieved inhibitory constraints imposed by *Pf*ODC on the *Pf*AdoMetDC domain and this resulted in higher activity. Alternatively, in the absence of kinetic data it can be speculated that peptide binding could have resulted in an altered K_m and/or better substrate accessibility to the catalytic site, which increased the catalytic efficiency of the *Pf*AdoMetDC enzyme. However, with the charge complement LE-21 peptide, the significant increase in *Pf*AdoMetDC activity could be due to prevention of the interaction of the α-helix within the O1 insert to this protein resulting in increased activities.

2.5. Conclusion

The results indicate that *Pf*ODC constrain the activity of *Pf*AdoMetDC in the bifunctional complex whereas *Pf*AdoMetDC is required for the optimal activity of *Pf*ODC [103]. These effects are mediated by protein-protein interactions, which could be similar in mechanism to that observed for antizyme and mammalian ODC [162] as well as prozyme and trypanosomal AdoMetDC [163,164]. The peptide probe studies showed that interference with the interaction sites of the O1 insert within the *Pf*ODC domain decreased its activity while *Pf*AdoMetDC activity was increased, indicative of a relieve of constraint placed on the *Pf*AdoMetDC domain by *Pf*ODC. The *Pf*ODC domain of *Pf*AdoMetDC/ODC may therefore coordinate the activities of both the domains within the bifunctional complex through long-range interdomain protein-protein interactions to simultaneously supply dcAdoMet and putrescine. In turn, investigations into the *Pf*AdoMetDC domain to identify specific features that mediate possible regulatory effects within the bifunctional protein should be performed. Together these results could provide an explanation for the evolutionary advantage of maintaining such a large open reading frame in the plasmodial genome. The bifunctional arrangement of *Pf*AdoMetDC/ODC is also reminiscent of the essential protein-protein interactions involved in the *Pf*DHFR/TS bifunctional protein in which the C-terminally located TS is dependent on the presence of the N-terminal DHFR domain [122]. Additionally, such a fusion of genes that encode two proteins linked with a hinge region enhances the effective concentration of protein domains that are involved in a common

metabolic pathway with respect to each other [174].

These studies are revealing the regulatory mechanisms employed by plasmodia to maintain optimum levels of the essential polyamines. Advances are therefore being made towards the identification of areas amenable to polyamine biosynthesis inhibition or uncoupling of the methionine and polyamine biosynthesis, essentially joined by the bifunctional *Pf*AdoMetDC/ODC complex, which could hopefully interfere with parasite survival.